JOURNAL OF CATALYSIS **168,** 431–441 (1997)
ARTICLE NO. CA971658

Influence of the Preparative Method on the Activity of Highly Acidic WO_x/ZrO_2 and the Relative Acid Activity Compared with Zeolites

J. G. Santiesteban,[1,2] J. C. Vartuli, S. Han, R. D. Bastian,[2] and C. D. Chang[1]

Mobil Technology Company, Paulsboro Technical Center, Paulsboro, New Jersey 08066-0480

Received October 10, 1996; revised February 4, 1997; accepted February 18, 1997

The acid activity of the solid tungsten/zirconia can be affected by the catalyst preparation method. Reflux of the hydrous zirconia prior to tungsten impregnation gives a catalyst with higher surface area than the nonrefluxed material, 62 vs 32 m^2/g, but with the same strong acid site density, as determined by *n*-pentane isomerization activity. It is also shown that the simultaneous coprecipitation of tungsten with the formation of hydrous zirconia yields a catalyst with about two times the strong acid site density of WO_x/ZrO_2 catalysts prepared by impregnation. Catalytic titration experiments using 2,6-dimethylpyridine reveal a distribution of strength of Brønsted acid sites, with a strong acid site density responsible for pentane isomerization activity of these materials of approximately 0.002 meq H^+/g catalyst for materials prepared by impregnation versus 0.004 meq H^+/g catalyst for catalysts prepared by coprecipitation. These strongly acidic sites are estimated to be about four orders of magnitude more active for pentane isomerization than the sites present in zeolite β. XPS of chemisorbed 2,6-dimethylpyridine and pyridine on the WO_x/ZrO_2 prepared by coprecipitation also indicates the presence of strong and weak Brønsted sites and Lewis acid sites. Weak Brønsted acid sites are predominant on the surface of the catalyst. The concentration of the different acid sites, as determined by XPS, is 0.013 meq Lewis acid sites/g catalyst, 0.011 meq strong Brønsted sites and 0.043 meq weak Brønsted sites. Further experimental work combining various characterization techniques with kinetic studies is needed to elucidate whether the Lewis acid sites play any role in the remarkable catalytic activity exhibited by these materials. The acid activity of WO_x/ZrO_2 catalysts has a strong dependence on the tungsten loading. The acid activity, as measured by *n*-pentane isomerization activity, passes through a maximum at approximately 16 wt% W loading. This amount represents about two monolayers coverage, assuming tungstate oxyanions, $WO_4^=$, on the surface of zirconia and is equivalent to the optimum atomic level of $SO_4^=$ needed for high acid activity suggesting that the site configuration may also be similar. © 1997 Academic Press

1. INTRODUCTION

Acid catalysis is the backbone of the petroleum and chemical processing industries. Environmental concerns and corrosion problems caused by the use of liquid acids and halogen-containing solid acids have created a need for highly acidic, environmentally friendly, and more stable solid acids. Zeolites, which have been extensively studied and used as catalysts in many processes, are not sufficiently acidic to replace liquid-phase systems (HF, H_2SO_4, BF_3) and/or halogen-containing solids (for example, chlorinated alumina) in processes where lower operating temperature may be advantageous to obtain the desired product. Some examples are isomerization of alkanes, isobutane alkylation, aromatic alkylation, olefin oligomerization, and a variety of aromatic acylation processes. Zeolites, and specifically zeolite β, have been used for the isomerization of paraffins such as heptane (1). However, the required higher operating temperature is less favorable for branched paraffin products and more favorable for cracked products. Sulfated zirconia catalysts, first reported by Holm and Bailey (2) in 1962 and later studied in detail by Japanese researchers (3–5), have received a great deal of attention because of their presumably high acidity and activity for the isomerization of paraffins, specifically *n*-butane, at low temperature. However, it appears that this catalyst system ages rapidly and irreversibly in a reducing atmosphere under commercial operating conditions.

Arata and Hino (6, 7) found that impregnation of hydrated zirconia, $ZrO(OH)_2 \cdot nH_2O$, with aqueous ammonium metatungstate followed by calcination in air at high temperatures (1073–1123°K) leads to the formation of strong acid sites on the tungsten oxide/zirconia catalyst as measured by Hammett indicators ($H_0 < -14.52$). These authors reported that a hydrous zirconia precursor is required for the anchoring of tungstate anions; if crystalline zirconia was used for the catalyst preparation or if the calcination temperature was not sufficiently high, $\geq$1073°K, before the tungstate impregnation, no superacid activity was observed. They concluded that tungsten oxide combines with zirconium oxide to create superacid sites at the time when zirconia is going through a phase transformation from amorphous to tetragonal.

In this paper, we compare the paraffin isomerization activity of zeolite β with that of tungsten oxide/zirconia catalysts, denoted in this paper as WO_x/ZrO_2, prepared by

[1] To whom correspondence should be addressed at present address.
[2] Present address: Air Products and Chemicals, Inc., 7201 Hamilton Boulevard, Allentown, PA 18195-1501. Fax: (610) 481-7719. E-mail: santiejg@apci.com.

0021-9517/97 $25.00
Copyright © 1997 by Academic Press
All rights of reproduction in any form reserved.

several methods. We observe that a preparation method which involves the simultaneous coprecipitation of tungsten with the formation of the hydrous zirconia yields a catalyst with about a twofold increase in strong acid site density as compared to catalysts prepared by tungsten impregnation of hydrous zirconia. Catalytic titration studies, using 2,6-dimethylpyridine as the titrant, were performed to determine relative strength and acid site density of WO_x/ZrO_2 catalysts prepared by different methods. These catalytic titration experiments also enabled us to estimate *n*-pentane isomerization forward rate constants based on number of active acid sites, i.e., turnover frequency. Comparison of these turnover frequencies with those estimated from zeolite β indicated that the acid sites on WO_x/ZrO_2 are about four orders of magnitude more active than those present in zeolites. X-ray photoelectron spectroscopy (XPS) of chemisorbed 2,6-dimethylpyridine and pyridine is used in some instances to complement the information obtained in the catalytic titration experiments. We also describe the acid activity of the improved WO_x/ZrO_2 catalyst prepared by coprecipitation as a function of tungsten loading.

2. EXPERIMENTAL

2.1. Catalyst Preparation

2.1.1. WO_x/ZrO_2 prepared by impregnation. This catalyst was prepared according to the procedure given by Arata and Hino (6, 7). Briefly, $Zr(OH)_4$ was prepared by dissolving 300 g of $ZrOCl_2 \cdot 8H_2O$ (Aldrich) in 4.5 L of distilled deionized water. A 10 *M* NH_4OH solution was added to precipitate out the $Zr(OH)_4$. The final pH of the mixture was approximately 9. The precipitate was filtered and washed with distilled water and then dried overnight at 368°K. $Zr(OH)_4$ was impregnated, using incipient wetness impregnation, with an ammonium metatungstate [$(NH_4)_6 \cdot H_2W_{12}O_{40} \cdot nH_2O$, Aldrich)] solution, to a 15 wt% tungsten target loading. The resulting material was air dried overnight at 368°K and then calcined at 1098°K in flowing dry air for 3 h. This catalyst is denoted IM.

2.1.2. WO_x/ZrO_2 prepared by refluxing $ZrO(OH)_2 \cdot nH_2O$ prior tungsten impregnation. $ZrO(OH)_2 \cdot nH_2O$ prepared according to the procedure described above was reslurried in excess water and then the pH was adjusted to ~9.0 with a 10 *M* NH_4OH solution. The resulting slurry was refluxed overnight and then cooled to room temperature, filtered, washed with water, and dried overnight at 368°K. Tungsten was added to the refluxed $ZrO(OH)_2 \cdot nH_2O$ by incipient wetness impregnation using an ammonium metatungstate solution, 15 wt% tungsten target loading. The resulting material was processed to the calcined form as described above. This catalyst is denoted R/IM.

2.1.3. WO_x/ZrO_2 prepared by coprecipitation. A solution of $ZrOCl_2 \cdot 8H_2O$ (Aldrich) was combined with stirring to a solution containing ammonium metatungstate and ammonium hydroxide. The pH of the resulting slurry was approximately 9.0. This slurry was placed in a steambox at ~100°C for 16 h. The product was recovered by filtration, washed with excess water, and dried overnight at 368°K. The material was processed to the calcined form as describe above. This catalyst is denoted COP.

2.1.4. Zeolite β. The zeolite $\beta(SiO_2/Al_2O_3 = 35/1)$ preparation procedure is described elsewhere (8). The proton (H-β) form was obtained by dry air calcination (810°K, 6 h) of the ammonium form (NH_4-β). MAS[27] Al-NMR confirmed that only tetrahedral aluminum was present.

2.2. Characterization

Powder X-ray diffraction spectra were collected on a Scintag XDS 2000 diffractometer using Cu*K*α radiation. Surface areas were determined by a multipoint BET measurement using nitrogen adsorption. Chemical analysis of the samples was carried out at Galbraith Laboratories.

X-ray photoelectron spectroscopic analyses of chemisorbed 2,6-dimethylpyridine and pyridine on WO_x/ZrO_2 were performed at Evans East Specialists in Materials Characterization. The XPS spectrometer used was a Perkin–Elmer, PHI Model 5000 LS XPS fitted with a monochromatic Al*K*α radiation (1486.6 eV) X-ray source, under a residual pressure of $\sim 10^{-8}$ Torr. The size of the analysis region was 3×1 mm. Charge effects were compensated for by the use of a flood gun. Binding energies were determined by reference to the $Zr(3d_{5/2})$ photoelectron line (182.2 eV). The hemispherical analyzer functioned in constant pass energy equal to 35.75 eV for high resolution spectra. High resolution spectral bands were deconvoluted into bands (90% Gaussian, 10% Lorentzian) with standard software, ACESS, from Perkin–Elmer using an integrated background subtraction. Before the impregnation with the organic base, the WO_x/ZrO_2 catalysts were pretreated at 773°K in flowing dry air for 1 h, to ensure removal of adsorbed water and organic contaminants, and then cooled to room temperature under flowing dry nitrogen. The samples were quickly immersed into a solution of pyridine or 2,6-dimethylpyridine dissolved in pentane to avoid exposure to air. While the pentane was gently stirred, it was allowed to evaporate at room temperature under nitrogen atmosphere. The WO_x/ZrO_2 samples impregnated with pyridine or 2,6-dimethylpyridine were transferred to a reaction vessel, which was connected to the high vacuum chamber of the XPS spectrometer, to be pretreated at 573°K, heating rate ~2°K/min, for 14 h under a 12 ml/min flow of dry nitrogen. This pretreatment was done to ensure homogeneous distribution of the organic base on the catalyst surface. The pretreatment time, 14 h, was determined during the catalytic titration experiments described below. After the pretreatment was performed, the sample was transferred

from the reaction vessel, without air exposure, to the vacuum load-lock and then to the XPS spectrometer.

2.3. Catalyst Testing

n-Pentane isomerization was used to determine acid activity of the various catalyst samples. The catalytic testing was carried out in a down-flow fixed-bed stainless-steel reactor. Catalyst samples were crushed and sieved to retain 14/30 mesh particle size. The catalyst was positioned in the central region of the reactor between two layers of sand (Fischer) and calcined at 773°K in flowing dry air for 1 h at atmospheric pressure to remove adsorbed water and/or adventitious carbon. After catalyst pretreatment, the reactor was cooled to ambient temperature and the unit was pressurized with hydrogen (Matheson, UHP) to 350 psig. *n*-Pentane (Aldrich, >99%) was fed into the reactor using a high pressure ISCO pump. Hydrogen and *n*-pentane flow rates were adjusted to give a 2 H_2/*n*-C_5 mol ratio. The temperature was then gradually increased to the desired operating temperature. After the Grove loader, the reactor effluent was diluted with nitrogen, and the combined stream was sent to on-line gas chromatography (GC) sampling for analysis. A fused silica capillary column (DB-1, 60 m) run isothermally at 293°K was used to determine product composition. Heating and insulating tapes were wrapped around the stainless-steel exit lines connected to the gas chromatograph to maintain temperature about 433°K to avoid condensation of the reaction products.

Isomerization forward areal rate constants were calculated assuming a first order reversible reaction and reported as molecules of *n*-pentane isomerized per unit surface area per unit time. Liquid hourly space velocity (LHSV) is defined as the volume of *n*-pentane (ml) contacting a given volume of catalyst (ml) in 1 h at STP. Likewise, weight hourly space velocity (WHSV) is defined as the weight of *n*-pentane (g) contacting a given catalyst weight (g) in 1 h at STP.

2.4. Titration of WO_x/ZrO_2 with 2,6-Dimethylpyridine

Mesh size particles (14/30) of WO_x/ZrO_2 were impregnated with 2,6-dimethylpyridine dissolved in pentane according to the following procedure. Prior to impregnation, the catalyst was pretreated at 773°K in flowing dry air for 1 h to ensure removal of adsorbed water and organic contaminants and then cooled to room temperature under flowing dry nitrogen. The catalyst was then quickly immersed into a solution of 2,6-dimethylpyridine dissolved in dry pentane, avoiding exposure to air. While the pentane was gently stirred, it was allowed to evaporate at room temperature under nitrogen atmosphere. Catalytic testing was performed as described above. Once the catalytic activity was determined under steady-state conditions, the unit was depressurized, flushed out with nitrogen, and then heated to 573°K, heating rate 2°K/min, in 10 ml/min of flowing dry nitrogen for a given time. This pretreatment was performed to ensure homogeneous distribution of the organic base on the catalyst surface. After this pretreatment, the unit was pressurized with hydrogen and the catalytic activity determined. This step was repeated until no redistribution of initially adsorbed 2,6-dimethylpyridine from inactive to active sites took place; this was reflected by constant catalytic activity.

3. RESULTS AND DISCUSSION

3.1. Catalyst Characterization

Table 1 shows the elemental analyses and surface area of the WO_x/ZrO_2 catalysts prepared by the different methods.

Overnight reflux of hydrous zirconia, $Zr(OH)_4$, with NH_4OH solution produces a catalyst with greater surface area, ~400 m^2/g, relative to the non-refluxed $Zr(OH)_4$, ~250 m^2/g. After tungsten impregnation and calcination, the refluxed material, denoted as R/IM, maintains a higher surface area, 62 m^2/g, than that of the nonrefluxed catalyst 32 m^2/g.

The results in Table 1 also indicate that the WO_x/ZrO_2 catalyst prepared by coprecipitation, denoted as COP, exhibits a surfaces area, 62 m^2/g, identical to that obtained on the catalyst prepared by refluxing $Zr(OH)_4$.

Structure determinations of the WO_x/ZrO_2 catalysts were made by X-ray powder diffraction. The results, Fig. 1, reveal that the COP catalyst contains only the tetragonal phase of zirconia (JCPDS-ICDD 24-1164). These results also suggest that the tungsten oxide species in the COP material exist mainly in an amorphous, noncrystalline state or as small crystallites of $\leq$5 nm diameter. Traces of monoclinic zirconia (JCPDS-ICDD 37-1484) are observed in the R/IM catalyst. Also, the peaks corresponding to tungsten oxide crystallites become more apparent in the R/IM catalyst. The IM catalyst exhibits a similar XRD pattern to that of the R/IM material with peaks higher intensity associated with the monoclinic zirconia phase and tungsten oxide crystallites.

TABLE 1

Elemental Analyses and BET Surface Areas of WO_x/ZrO_2 Catalysts

Catalyst: Preparation method:	IM Impregnation	R/IM Refluxed/ impregnation	COP Coprecip- itation
Elemental analyses (wt%)			
W	15.0	16.9	15.5
Zr	63.2	61.4	63.4
Ash, 1000°C	—	—	99.6
BET surface area, before calcination (m^2/g)	250	400	—
BET surface area (m^2/g)	31	62	62

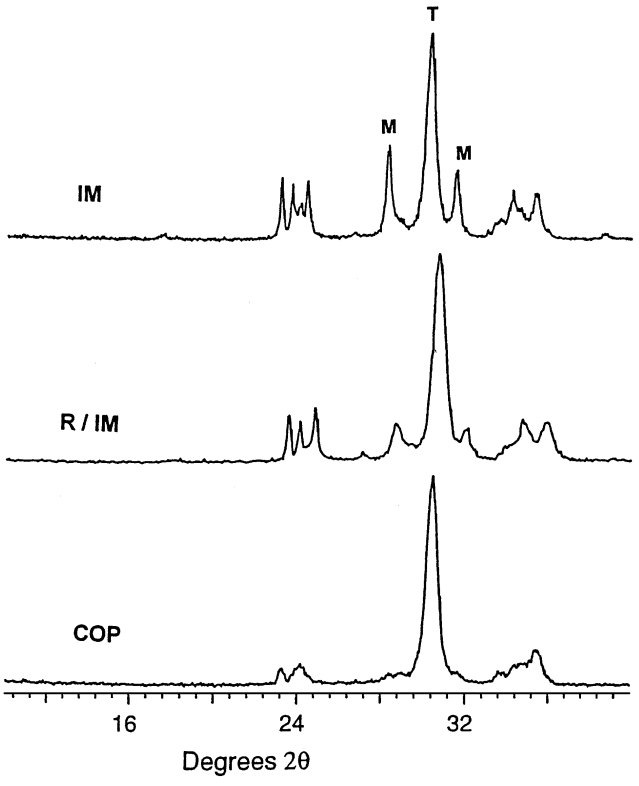

FIG. 1. X-ray diffraction patterns of WO_x/ZrO_2 catalysts prepared by impregnation (IM), refluxed/impregnation (R/IM), and coprecipitation (COP).

The stabilization of the tetragonal zirconia phase upon heating zirconium hydroxide in contact with tungsten oxo-species is consistent with Arata and Hino findings (6). This stabilization effect, as well as other effects such as retardation of the process of crystallization of zirconium hydroxide to the tetragonal phase and tetragonal-monoclinic phase transition, has also been reported to take place with the incorporation of numerous metal oxides such as MgO, CaO, Sc_2O_3, Y_2O_3, La_2O_3, CeO_2, etc. (9–11). The details of the mechanism governing the stabilization process are still a matter of controversy (12). It has been shown that tetragonal zirconia is stabilized with a small crystallite size due to its lower surface tension than in the monoclinic form (13). Thus, one could propose that the interaction of tungstate anions with the hydroxyl groups of hydrous zirconia not only retards the crystallization process but also inhibits sintering of zirconia crystallites favoring the stabilization of the tetragonal phase.

3.2. *n*-Pentane Isomerization

Isomerization of *n*-pentane to isopentane was chosen as a test reaction to determine the relative acid activity of the different WO_x/ZrO_2 catalysts. Total product distribution and isomerization rates obtained over these catalysts are given in Table 2. No catalyst deactivation was observed during the test period, 2–3 days, for these catalysts. The data presented in Table 2 were obtained after approximately 40 h on stream. The isomerization data were interpreted kinetically in terms of a reversible first-order reaction, for which the integrated rate expression is

$$-\ln(1 - X/X_e) = k_A(t/X_e) \quad \text{or}$$
$$k_A = (1/t)(X_e)[-\ln(1 - X/X_e)],$$

where X_e is the equilibrium conversion, $1/t$ is the superficial contact time in molecules of *n*-C_5 feed/cm^2 of catalyst · s, and k_A is the forward areal rate constant in molecules of *n*-C_5 isomerized/cm^2 of catalyst · s. The equilibrium conversion at 483°K is 74.2% *i*-C_5/total C_5's. This value was estimated in our laboratory, and is in agreement with that reported by others (14).

For practical purposes, forward isomerization rates based on mass (k_w) and volume (k_v) are also given in Table 2. Liquid hourly space velocity is defined as the volume on *n*-pentane (ml) contacting a given volume of catalyst (ml) in 1 h at standard temperature and pressure. Thus, the units for k_v are milliliters of pentane per milliliter of catalyst per hour. Likewise, weight hourly space velocity is defined as

TABLE 2

***n*-Pentane Conversion over WO_x/ZrO_2 Catalysts at 483°K, 2 H_2/*n*-C_5 molar ratio, 2 LHSV (ml *n*-C_5/ml cat · h), and 350 psig**

Catalyst: Preparation method:	IM Impregnation	R/IM Refluxed/ impregnation	COP Coprecipitation
BET surface area (m^2/g)	32	62	62
Catalyst weight (g)	6.2	6.0	4.8
Catalyst volume (ml) (14/30 mesh)	4.0	5.0	4.0
LHSV	2.0	2.0	2.0
WHSV	0.81	1.04	1.04
Product distribution (mol%)			
CH_4	0.09	0.22	0.59
C_2H_6	0.17	0.33	0.66
C_3H_8	0.20	0.34	0.72
i-C_4H_{10}	0.77	1.23	3.67
n-C_4H_{10}	0.12	0.17	0.27
i-C_5H_{12}	55.7	61.0	68.3
n-C_5H_{12}	42.1	35.6	25.2
C_6's	0.85	1.01	0.63
i-C_5/total C_5's (%)	56.9	63.2	73.1
Total cracking products C_4^- (mol%)	0.93	1.60	5.91
Forward areal rate constant (k_A)	6.46×10^{12}	5.54×10^{12}	12.1×10^{12}
$k_v = (\text{LHSV})(X_e) \cdot [-\ln(1 - X/X_e)]^a$	2.16	2.83	6.22
$k_w = (\text{WHSV})(X_e) \cdot [-\ln(1 - X/X_e)]^a$	0.88	1.47	3.24

[a] $X_e = 0.742$.

the weight of pentane (g) contacting a given catalyst weight (g) in 1 h at standard temperature and pressure. Units for k_w are grams of *n*-pentane per gram of catalyst per hour.

Comparison of the forward areal rate constants (k_A) (15), defined as molecules of *n*-pentane isomerized per unit surface area per second, among the catalysts indicates that the acid site density of the WO_x/ZrO_2 catalysts prepared by coprecipitation, COP, is at least two times higher than that of the catalysts prepared by impregnation, IM, and refluxed/impregnation, R/IM. Notice that the %*i*-C_5/total C_5's value of the COP catalyst is very close to equilibrium and one could argue that the forward isomerization rate constant for the COP catalyst may be underestimated. A better estimate of the difference in acid site density between the COP and R/IM materials is obtained from our catalytic titration data that are discussed in the following section. These results revealed that the strong acid site density of the COP catalyst is about twice that of the R/IM material. We propose that the higher acid site density of the COP material is due to a larger number of tungstate ions interacting with the hydoxyl groups of the $Zr(OH)_4$ formed during the coprecipitation step.

The higher acid activity of the COP material is also reflected in the formation of higher amounts of cracked products, C_4^-. It is worthwhile to mention that the cracked product distribution indicates that these products are mainly formed via oligomerization-β scission processes involving carbenium ion chemistry, i.e., acid catalysis. This is reflected, for example, by the higher selectivity of isobutane compared to butane. Carbenium ion chemistry favors the formation of tertiary fragments, precursors of isobutane, over the formation of secondary or primary ion fragments, precursors of *n*-butane (16, 17). In addition, the moles of butanes formed exceed those of methane, the other expected product of direct pentane cracking.

To gain insight into the number of acid sites responsible for the remarkable acid activity of the tungsten/zirconia catalysts, we performed a series of catalytic titration experiments using 2,6-dimethylpyridine. The results are discussed in the following section.

3.3. Catalytic 2,6-Dimethylpyridine Titration

The number of acid sites on solid catalysts can be determined by the amount of amine required to poison the catalytic activity for a model reaction as reported by Mills *et al.* (18). This technique has been applied by many authors to determine not only the number of sites, but also the nature and strength of the acid sites involved in catalytic reactions (19). The main issue when performing catalytic titration experiments is to ensure the homogeneous distribution of the poison over the catalyst surface, i.e., to ensure that the titrant represents the minimum amount of catalyst poison. When the poison is an organic base such as an amine, an adequate temperature pretreatment may allow the amine to diffuse on the catalyst surface from inactive to active acid sites. But, even after the poisoning effectiveness is optimized by temperature redistribution treatments, a considerable fraction of the amine can remain coordinatively bound to Lewis acid sites, which are generally considered not to be direct participants in hydrocarbon transformations, although they may dramatically increase the strength of Brønsted sites via inductive effects (20). Thus, it is also necessary to use an amine for the selective titration of Brønsted acid sites in the presence of Lewis sites. Sterically hindered amines such as 2,6-dimethylpyridine were earlier suggested by Brown and Johanneson (21), and later applied by other authors (e.g., 19, 22) as selective probes for Brønsted sites; the position of the methyl groups hinders coordination of the nitrogen atoms with Lewis acid sites.

Before we describe the catalytic titration results, let us discuss briefly the optimization of the pretreatment procedure. Table 3 summarizes the results obtained during optimization of the pretreatment procedure of the R/IM WO_x/ZrO_2 catalyst impregnated with 2,6-dimethylpyridine. The data indicate that a 13-h pretreatment at 573°K was required to ensure that 2,6-dimethylpyridine was chemisorbed on catalytically active acid sites. Kjeldahl nitrogen analyses performed at Galbraith Laboratories of the sample before and after pretreatment indicate no loss of 2,6-dimethylpyridine to the gas phase during the pretreatment procedure.

Figure 2 depicts the catalytic titration results of *n*-pentane isomerization obtained over the R/IM and COP catalysts. The shape of the curves suggests that there is a distribution of strength of acid sites, or at least two sites with different acid strength, present on these catalysts. The slope of the activity versus the amount of 2,6-dimethylpyridine in the catalyst allows us to assess the acid strength; the number or density of strong acid sites responsible for most of the activity can be estimated from the initial slope of the curves. Results from Fig. 2 also revealed that the amount of 2,6-dimethylpyridine required to poison all the catalytic activity is comparable for both catalysts. This result suggests that

TABLE 3

Effect of Pretreatment on the Activity of R/IM Catalyst Doped with 230 ppm of 2,6-Dimethylpyridine for Pentane Isomerization

Total pretreatment time (h)	*i*-C_5/total C_5's (%)	Forward areal rate constant (k_A) ($\times 10^{12}$ molecules *n*-C_5/cm^2 · s)
1	45.82	2.77
13	28.92	1.43
20	29.00	1.43

Note. Pretreatment conditions: 573°K in flowing nitrogen (10 ml/min). Reaction conditions: 483°K, 2 H_2/*n*-C_5 molar ratio, 350 psig, and 2 LHSV (ml *n*-C_5/ml cat · h) or 1.04 WHSV (g *n*-C_5/g cat · h).

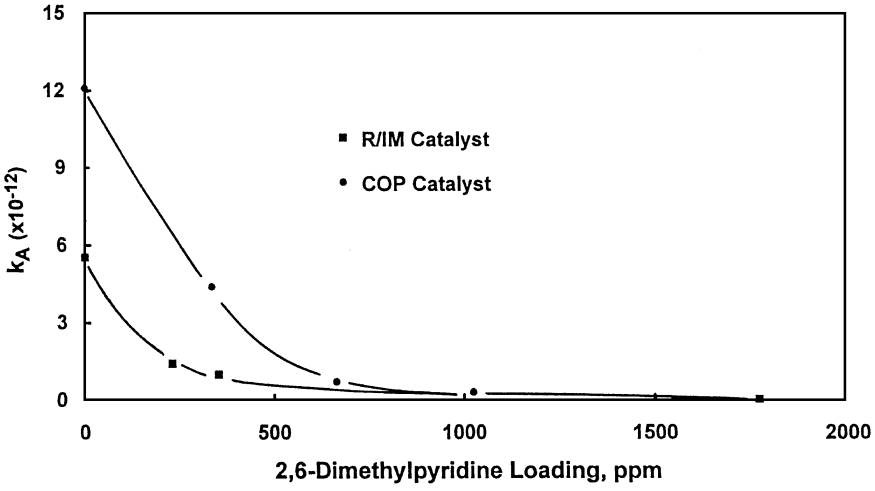

FIG. 2. *n*-Pentane isomerization activity of WO_x/ZrO_2 catalysts prepared by refluxed/impregnation (R/IM) and coprecipitation (COP) after titration with 2,6-dimethylpyridine. Reaction conditions are given in Table 3.

the total number of acid sites, strong and relatively weak, is similar in both catalysts, with the COP catalyst having approximately twice the number of strong sites than those present in the R/IM material. The results are summarized in Table 4. It is quite remarkable that such a small number of acid sites is responsible for the high activity exhibited by these materials.

In an attempt to estimate the strength difference between the acid sites present on WO_x/ZrO_2 and those present in zeolites, we performed pentane isomerization experiments over a zeolite β at operating conditions similar to those used for WO_x/ZrO_2 catalysts and compared their respective turnover frequencies. The results are discussed in the following section.

3.4. Comparison of Turnover Frequency between WO_x/ZrO_2 and Zeolite β

The data in Table 5 indicate that zeolite β ($SiO_2/Al_2O_3 = 35$) is not active for *n*-pentane isomerization at 483°K, with only about 1 wt% isopentane obtained. Even at 533°K the isopentane yield is a fraction of that obtained over the WO_x/ZrO_2 catalyst at 483°K.

TABLE 4

Density of Strong and Total Brønsted Acid Sites Participating in the *n*-Pentane Isomerization as Determined by Catalytic Titration using 2,6-Dimethylpyridine

Catalyst	Strong Brønsted sites			Total Brønsted sites (meq/g cat)
	2,6-DMP, ppm	meq/g cat	2,6-DMP, ppm	
R/IM	0.22	2.0×10^{-3}	≤1.0	$\leq 9.4 \times 10^{-3}$
COP	0.43	3.9×10^{-3}	1.0	9.4×10^{-3}

Table 6 shows the estimated turnover frequency (molecules converted per active acid site per second) for WO_x/ZrO_2 and zeolite β. The number of acid sites in WO_x/ZrO_2 was estimated from the catalytic titration experiments (Table 4). For zeolite β, it was assumed that all the tetrahedral aluminum, as determined by ^{27}Al NMR, was participating in the reaction (23). The turnover frequency results imply that the acid sites on WO_x/ZrO_2 are about four orders of magnitude more active than those present in the zeolite β for paraffin isomerization. Accepting for the moment the Hammett acidity value ($H_0 < -14.52$) for activated WO_x/ZrO_2 given by Hino and Arata (6, 7), this

TABLE 5

***n*-Pentane Conversion over Zeolite β at Two Different Temperatures, 483 and 533°K, 2 H_2/*n*-C_5 molar ratio, and 350 psig**

Temperature (°K)	483	533
Catalyst weight (g)	2.2	2.2
Catalyst volume (ml) (14/30 mesh)	4.0	4.0
LHSV (ml *n*-C_5/ml cat · h)	2.0	2.0
WHSV (g *n*-C_5/g cat · h)	2.28	2.28
Product distribution (mol%)		
CH_4	—	0.05
C_2H_6	—	0.02
C_3H_8	—	0.03
i-C_4H_{10}	—	0.09
n-C_4H_{10}	—	0.04
i-C_5H_{12}	1.10	10.8
n-C_5H_{12}	98.9	88.7
C_6's	—	0.21
i-C_5/total C_5's (%)	1.10	10.9
Total cracking products C_5^- (mol%)	—	0.22
$k_v = (\text{LHSV})(X_e)[-\ln(1 - X/X_e)]$	0.02	0.24
$k_w = (\text{WHSV})(X_e)[-\ln(1 - X/X_e)]$	0.02	0.27

TABLE 6

Relative Turnover Frequencies of WO_x/ZrO_2 Catalysts (R/IM and COP) and Zeolite β for *n*-Pentane Isomerization at 483°K, 350 psig, 2 H_2/n-C_5 molar ratio, and 2 LHSV (ml n-C_5/ml cat · h)

Catalyst	meq H^+/g catalyst	Turnover frequency	Relative turnover frequency
β Zeolite	0.9	8.72×10^{-5} 1.15×10^{-3} (at 533°K)	1 13
WO_x/ZrO_2 (R/IM)	0.002	2.8	32,000
WO_x/ZrO_2 (COP)	0.0042	3.9	44,000

difference in activity would imply that the acidity of zeolite β is similar to ~90% H_2SO_4. This is in general accord with the ranking of solid acids devised by Haw *et al.* (24), based on the acid strength of carbocations and other electrophiles in various media. It should be noted, however, that in the case of sulfated zirconia, which also catalyzes *n*-alkane isomerization, there is increasing evidence that its acidity does not exceed that of 100% H_2SO_4 (25, 26).

The turnover frequency of the WO_x/ZrO_2 catalysts prepared by different methods, refluxed/impregnation (R/IM) and coprecipitation (COP), are similar. This result suggests that the nature of sites present on these materials are alike, and the difference in activity is due to a higher density of acid sites on the COP catalyst relative to the R/IM catalyst.

It is important to mention that under the isomerization conditions used in the present study, WO_x/ZrO_2 does not exhibit any hydrogenation/dehydrogenation activity. Thus, the *n*-pentane isomerization activity of this material is solely due to the highly acidic sites. *n*-Pentane isomerization is taking place only via intermolecular hydride transfer catalyzed by strong acid sites.

3.5. X-Ray Photoelectron Spectroscopy of Chemisorbed Pyridine and 2,6-Dimethylpyridine over WO_x/ZrO_2

The potential of XPS to study the nature and strength of acid sites present in zeolite Y by determining the position and intensity of the N1*s* XPS peak of an adsorbed organic base was demonstrated in the 1970s by Defosse and Canesson (27, 28). Since then, several workers have extended the use of this technique for the study of other zeolitic materials (29–31). XPS should be a suitable technique to determine nature (Brønsted and/or Lewis) and relative strength of acid sites of these mixed metal oxides because, unlike zeolites, the acid sites present on the relatively low surface area (~62 m^2/g) WO_x/ZrO_2 catalysts are on the external surface. In addition, semiquantitative information on the density of acid sites can be obtained with this technique. The XPS study of chemisorbed 2,6-dimethylpyridine and pyridine was used to complement the catalytic titration experiments discussed above.

Figure 3a shows the profile of the N1*s* XPS spectrum obtained on the COP catalyst doped with 2,6-dimethylpyridine (nominal concentration 0.3 wt%). The XPS spectrum contains two clearly distinct N1*s* peaks located at binding energies of 400.0 ± 0.2 eV and 401.8 ± 0.2 eV. These peaks can be assigned to nitrogen atoms of 2,6-dimethylpyridinium ions associated with relatively weak and strong Brønsted acid sites, respectively (31). The spectrum of Fig. 3a was obtained before the sample was pretreated (heated in low nitrogen flow at 573°K for 14 h). It was found that after the pretreatment, the relative intensity of the N1*s* peak located at 401.8 eV, assigned to the strong Brønsted acid site, increases with respect to the N1*s* peak located at 400 eV, assigned to weak Brønsted sites (Fig. 3b). The results are summarized in Table 7. The relative increase of nitrogen species interacting with strong Brønsted sites upon heating of the sample is attributed to redistribution of initially adsorbed 2,6-dimethylpyridine from weak to stronger acid sites and not to the loss to the gas phase of the organic base interacting with weak acid sites. This was corroborated by elemental analysis of the samples before and after pretreatment, as shown in Table 8. Furthermore, the migration of the 2,6-dimethylpyridine toward the strong acid sites was also observed during optimization of the pretreatment procedure for the catalytic titration experiments (see Table 3).

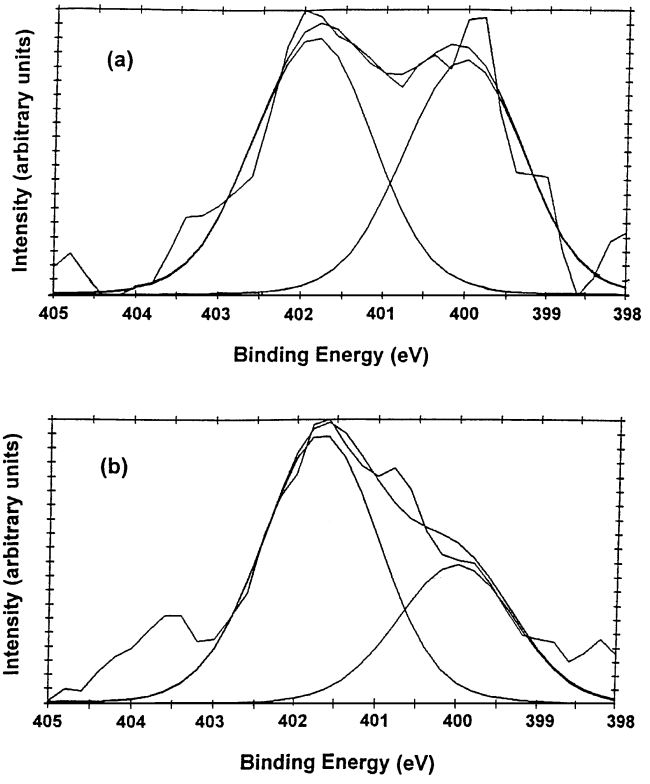

FIG. 3. N1*s* photoelectron spectra of 0.3 wt% (nominal concentration) 2,6-dimethylpyridine chemisorbed on WO_x/ZrO_2 (a) before pretreatment and (b) after pretreatment.

TABLE 7

Binding Energies and Relative Concentration of N1*s* Components of 2,6-Dimethylpyridine (0.3 wt% Nominal Concentration) Chemisorbed on WO_x/ZrO_2 Catalyst

	Before pretreatment		After pretreatment[a]		
	B.E. (eV)	Relative concentration	B.E. (eV)	Relative concentration	Acid site type
Peak I	401.8	52	401.7	66	Strong Brønsted
Peak II	400.0	48	400.0	34	Weak Brønsted

[a] Heating at 573°K for 14 h in flowing dry nitrogen (12 cc/min).

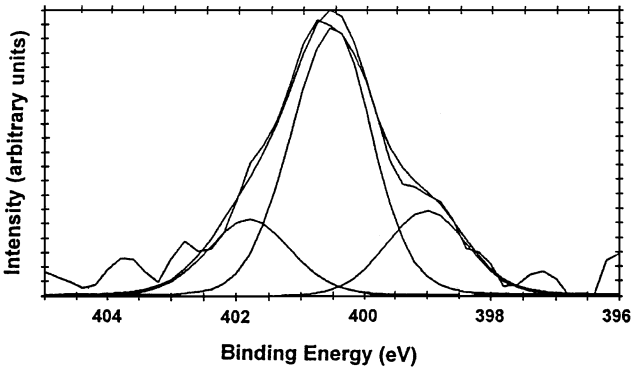

FIG. 4. N1*s* photoelectron spectra of 1.1 wt% (nominal concentration) 2,6-dimethylpyridine chemisorbed on WO_x/ZrO_2.

Another feature of the XPS results obtained on the chemisorption of 0.3 wt% 2,6-dimethylpyridine on WO_x/ZrO_2 (Fig. 3) is that there are no N1*s* peaks present that could be ascribed to 2,6-dimethylpyridine bound to Lewis sites. The N1*s* peak which is attributed to the interaction of the base with Lewis sites is observed only when higher concentrations of this sterically hindered organic base were used. This occurs at a binding energy of approximately 399 eV.

Figure 3B presents what seems to be a peak at ~403.6 eV. This feature could not be assigned to any reasonable nitrogen containing species. In addition, we tried unsuccessfully to deconvolute this feature.

Figure 4 shows the N1*s* XPS spectrum obtained on the WO_x/ZrO_2 catalyst containing a nominal concentration of 2,6-dimethylpyridine of 1.1 wt%. The presence of a shoulder peak to the main peak at low-binding-energy values, ~399.0 eV is apparent. This shoulder peak is assigned to the nitrogen of the 2,6-dimethylpyridine associated with Lewis sites (27, 30). In addition, the main N1*s* peak was found to be ~40% broader than those of the reference peaks, namely Zr3$d_{5/2}$ and Zr3$d_{3/2}$. Therefore, this main N1*s* peak was deconvoluted into two components with the same FWHM (full width at half-maximum) vlaue of 1.5 eV. The resulting binding energy of the main (400.5 ± 0.2 eV) and minor (401.8 ± 0.2 eV) peak components correspond to the nitrogen of 2,6-dimethylpyridinum ions associated with weak and strong Brønsted sites. The relative concentrations of the weak and strong Brønsted sites, along with the Lewis sites, are given in Table 9. Note that the relative concentrations of the various nitrogen species did not change significantly upon the heating pretreatment (573°K for 14 h in nitrogen flow). Elemental analysis indicated that ~30% of the total amount of 2,6-dimethylpyridine was lost during heat pretreatment/XPS analysis of the samples. The results are presented in Table 10 and suggest that physisorbed 2,6-dimethylpyridine on nonacidic sites may be lost during the heat pretreatment or high vaccum environment (10^{-8} Torr) of the XPS spectrometer. These results suggest that the 2,6-dimethylpyridine remaining on the catalyst, ~0.72 wt%, is bound only to acid sites. This amount represents about 1/3 monolayer coverage, taking into account that the surface area of the catalyst is 62 m^2/g and assuming a spherical diameter of 7.8 Å for the organic base.

The results presented in Table 9 also show that weak Brønsted sites are the predominant acid sites present on the WO_x/ZrO_2 surface. Comparison of Tables 7 and 9 suggests that interaction of the sterically hindered 2,6-dimethylpyridine with Lewis sites takes place only after all the acidic protons have been titrated. The specificity of the sterically hindered 2,6-dimethylpyridine for protons

TABLE 8

2,6-Dimethylpyridine Concentration on WO_x/ZrO_2 as Determined by Elemental Nitrogen Analysis

	Kjeldahl nitrogen[a] (ppm)	2,6-Dimethylpyridine (wt%)
As prepared	380 ± 30	0.29 ± 0.02
After heat pretreatment & after XPS analysis	430 ± 30	0.33 ± 0.02

Note. 2,6-Dimethylpyridine nominal concentration was 0.3 wt%.
[a] Analysis performed by Galbraith Laboratories Inc.

TABLE 9

Binding Energies and Relative Concentration of N1*s* Components of 2,6-Dimethylpyridine (1.1 wt% Nominal Concentration) Chemisorbed on WO_x/ZrO_2 Catalyst

	Before pretreatment		After pretreatment		
	B.E. (eV)	Relative concentration	B.E. (eV)	Relative concentration	Acid site type
Peak I	401.8	18	401.5	16	Strong Brønsted
Peak II	400.5	63	400.5	64	Weak Brønsted
Peak III	399.0	19	398.7	20	Lewis

TABLE 10

2,6-Dimethylpyridine Concentration on WO_x/ZrO_2 as Determined by Elemental Analysis

	Kjeldahl nitrogen (ppm)	2,6-Dimethylpyridine (wt%)
As prepared	1490 ± 20	1.14 ± 0.02
After heat pretreatment & after XPS analysis	950 ± 20	0.72 ± 0.02

Note. 2,6-Dimethylpyridine nominal concentration was 1.1 wt%.

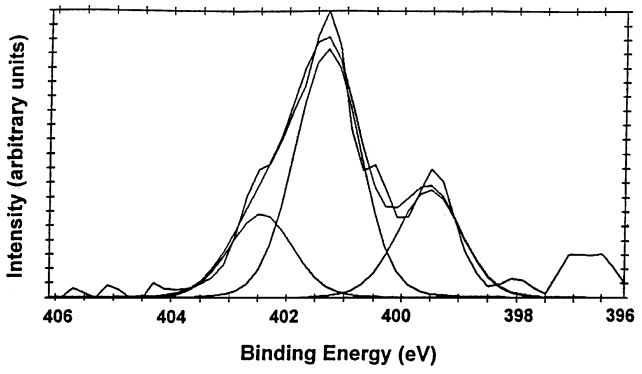

FIG. 5. N1*s* photoelectron spectra of 1.1 wt% (nominal concentration) pyridine chemisorbed on WO_x/ZrO_2.

was earlier suggested by Brown and Johanneson (21) and later applied by several authors (19, 22).

Since the catalysts lack microporosity, it is reasonable to assume that the acid sites are located solely on the surface of the catalyst. Thus, one can combine the N1*s* XPS information presented in Table 9 and the total amount of 2,6-dimethylpyridine determined to be present in the sample after pretreatment/XPS analysis (0.72 wt%), Table 10, to determine the acid site density of the different sites present on the catalyst. The results are presented in Table 11. It should be noted that the density of strong Brønsted sites, 0.011 meq/g catalyst, estimated from XPS is higher than that obtained from catalytic titration experiments, 0.004 meq/g catalyst (see Table 4). Also, the total amount of 2,6-dimethylpyridine associated with Brønsted acid sites, as determined by XPS, was much higher than that determined by the catalytic titration experiments, 0.57 wt% vs 0.01 wt%, respectively. Therefore, the XPS results should be taken with caution; although they are useful in determining the relative concentration of Brønsted and Lewis acid sites on the surface of the catalyst.

Since, as discussed above, the sterically hindered 2,6-dimethylpyridine is selective toward the interaction with Brønsted sites over Lewis sites, there was the question whether all the Lewis sites were titrated. To address this issue, we performed experiments using pyridine. The results are depicted in Fig. 5 and summarized in Table 12. The data indicate that weak Brønsted sites are the predominant acid sites (~60%) on the surface of the WO_x/ZrO_2 catalyst, and also that the concentration of strong Brønsted acid sites is close to the concentration of Lewis sites. These results are consistent with those obtained with high 2,6-dimethylpyridine loadings (Table 9).

It is also interesting to note in Tables 11 and 12 that the ratio of strong Brønsted acid sites to Lewis acid sites is close to 1. It would be appealing to suggest that the highly acidic activity of WO_x/ZrO_2 originates from a conjugate Brønsted–Lewis site. However, as discussed above, there is a discrepancy between the number of strong Brønsted sites determined by XPS and that determined by catalytic titration experiments. Nevertheless, it would be important to carry out more detailed experiments combining various characterization techniques with catalytic data to establish whether the high acid activity of these materials originates from a Brønsted–Lewis conjugate acid site.

3.6. Effect of W Loading

The effect of W loading in the catalytic activity of COP is depicted in Fig. 6. The *n*-pentane isomerization activity goes through a maximum as the tungsten loading increases. The activity is highest at approximately 16 wt% W. This effect of activity on tungsten loading agrees quite well with the earlier data by Arata (6) obtained on a catalyst prepared by impregnation. It is interesting to correlate our catalytic data with recent temperature-programmed reduction (TPR)

TABLE 11

Milliequivalents of the Various Acid Sites Present on WO_x/ZrO_2 as Determined by XPS of Chemisorbed 2,6-Dimethylpyridine

	meq/g of WO_x/ZrO_2
Strong Brønsted sites	0.011
Weak Brønsted sites	0.043
Lewis sites	0.013

TABLE 12

Binding Energies and Relative Concentration of N1*s* Components of Pyridine (1 wt% Nominal Concentration) Chemisorbed on WO_x/ZrO_2 Catalyst

	B.E. (eV)	Relative concentration	Acid site type
Peak I	402.4	19	Strong Brønsted
Peak II	401.3	57	Weak Brønsted
Peak III	399.5	24	Lewis

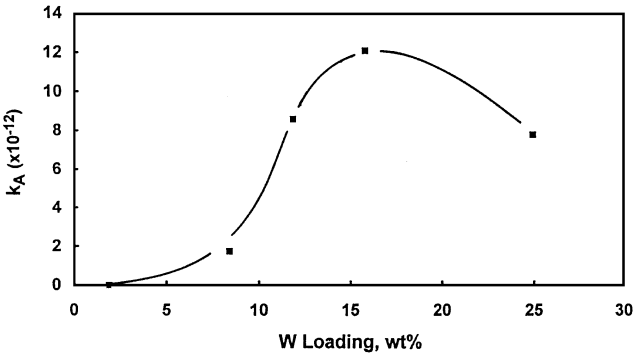

FIG. 6. *n*-Pentane isomerization activity of WO_x/ZrO_2 catalysts prepared by coprecipitation (COP) as a function of W loading. Reaction conditions 483°K, 2 H_2/n-C_5 molar ratio, 350 psig, and 2 LHSV (ml *n*-C_5/ml cat · h) or 1.04 WHSV (g *n*-C_5/g cat · h).

results (32) which indicate the reducibility of tungsten oxospecies on ZrO_2 was also dependent on the W loading level. At low tungsten loadings, ~2 wt% W, the tungsten oxospecies are reduced only at very high temperatures, >1073°K. At 8 wt% W loading (about a monolayer coverage, assuming surface WO_4^- species) tungsten oxospecies are reduced at lower temperatures, >873°K, but still slightly higher than that required for bulk-like WO_3. The difficulty in reducing tungsten oxospecies below or at monolayer coverage suggested a strong interaction between the tungsten oxospecies and the ZrO_2 support; similar results were reported in the tungsten oxide–alumina system (33). At 16 wt% W loading, approximately two times monolayer coverage, the reduction of tungsten oxospecies took place at two distinct temperature regions; about 10% of the tungsten oxospecies are reduced in the 640–670°K region, and the rest are reduced in the bulk-like WO_3 region, 800–920°K. It was suggested (32) that the former were participating in the formation of the highly acidic sites present on WO_x/ZrO_2. The suggestion was based on the observation that these materials lose some acid activity when exposed to relatively high reducing conditions.

The above results clearly indicate a correlation between reducibility of tungsten oxospecies and their catalytic acid activity. WO_x/ZrO_2 catalysts containing tungsten oxospecies difficult to reduce, i.e., less than a monolayer coverage, do not show high acid activity. Conversely, high acid activity is observed in WO_x/ZrO_2 catalysts containing tungsten oxospecies which are relatively easy to reduce, i.e, high W loadings, >12 wt% W.

The question to be addressed at this point is: what is the structure of the acid site responsible for the high activity of the WO_x/ZrO_2 catalyst? Catalytic titration experiments indicated that the improved WO_x/ZrO_2 catalyst prepared by coprecipitation, ~16 wt% W loading, contains approximately 0.004 meq H^+/g. If we assume that one W atom is associated with one acid site poisoned by 2,6-dimethylpyridine, it is estimated that only 0.072 wt% W/ZrO_2 are involved in the formation of the highly acidic sites. On the other hand, we found that a 2 wt% W/ZrO_2 catalyst contains no strong acid sites capable of carrying out pentane isomerization. Our results indicate that approximately 16 wt% W is required to maximize the acid site density of these materials (Fig. 6). Current models proposed in the literature cannot reconcile these results. Arata and Hino (6) attributed the strong acidity to a bidentate tungstate anion coordinated to the zirconia support, as that proposed in the sulfated zirconia system (34). Afanasiev *et al.* (35) proposed a model in which several tungsten oxoanions surround a hydrated zirconium oxide group, with OH groups attached to Zr atoms being responsible for the high acid activity of these materials.

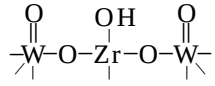

These models do not agree with our findings that W loadings well above a monolayer are needed to generate highly acidic sites. This is of course assuming that all of the tungsten is on the catalyst surface. This assumption is likely more valid for the catalysts prepared by impregnation than that of the coprecipitation method. In addition, it is expected that the tungsten oxospecies proposed in above models would be difficult to reduce owing to strong interaction with the zirconia support (32), and there are indications that relatively easy reducible tungsten oxospecies are responsible for the high acid activity exhibited by these materials. Bulk tungsten oxide and reduced tungsten oxides have been recognized (36–38) to have some acidity, but their activity per se would be too weak to explain our results.

Recently, Iglesia *et. al.* (39) suggested that the site configuration in tungstated zirconia does not consist of isolated tungstate groups. Based on their UV–visible spectroscopy and X-ray adsorption studies, Iglesia *et al.*, proposed that the active sites in tungstated zirconia consist of highly distorted octahedral WO_x clusters. This proposal seems to be consistent with the fact that optimum catalytic acid activity is obtained on samples with ~16 wt% W loading, about two monolayer coverage. However, direct evidence that these distorted octaheldral WO_x clusters are responsible for the remarkable high acid activity of these materials is lacking.

CONCLUSIONS

The study of the acid activity of the WO_x/ZrO_2 solid acid catalyst as a function of preparation method indicated several key findings. Refluxing of hydrous zirconia prior to tungsten impregnation yielded a catalyst with higher surface area, but with the same acid site density as those non-refluxed. Preparing WO_x/ZrO_2 catalyst by the simultaneous coprecipitation of tungsten with the formation of hydrous zirconia yielded a catalyst with two times

the strong acid site density compared to WO_x/ZrO_2 catalysts prepared by impregnation. Catalytic titration experiments indicated that the strong acid site density of these materials responsible for the high pentane isomerization activity was rather low; 0.002 meq H^+/g catalyst for materials prepared by impregnation versus 0.004 meq H^+/g catalyst for materials prepared by coprecipitation. The strong acid sites on WO_x/ZrO_2 were estimated to be about four orders of magnitude more active for *n*-pentane isomerization than those present in zeolite β. XPS of chemisorbed 2,6-dimethylpyridine and pyridine revealed the presence of Lewis acid sites as well as stong and weak Brønsted acid sites on the surface of the WO_x/ZrO_2 catalysts prepared by coprecipitation. XPS semiquantitative analysis combined with elemental nitrogen analysis indicated that 0.72 wt% 2,6-dimethylpyridine was the maximum amount of base interacting with the acid sites present on the WO_x/ZrO_2 surface. The results also indicated that weak Brønsted sites were the predominant acid sites (~60%) and that the approximate concentration of strong Brønsted acid sites was close to the concentration of Lewis sites (20%). In terms of milliequivalents of acid per gram of catalyst these amounts represented 0.013 meq Lewis sites, 0.011 meq strong Brønsted sites, and 0.043 weak Brønsted sites. From the catalytic activity viewpoint, these numbers must be taken with caution, since catalytic titration experiments, which give a better indication of the acid sites participating in the reaction, indicated a much lower Brønsted acid site density; i.e., 0.004 meq/g catalyst for strong Brønsted sites and 0.005 meq/g for weak Brønsted sites. It was found that ~16 wt% W loading was required to maximize the acid site density of the catalyst. This represented about two monolayers coverage. Further detailed characterization studies are needed to elucidate the structure of the highly acidic site present on WO_x/ZrO_2.

REFERENCES

1. Blomsma, E., Martens, J. A., and Jacobs, P. A., *J. Catal.* **159**, 323 (1996).
2. Holm, V. C. F., and Bailey, G. C., U.S. Patent 3,032,599, assigned to Phillips Petroleum, 1962.
3. Hino, M., and Arata, K., *J. Chem. Soc. Chem. Commun.* 851 (1980).
4. Yamaguchi, T., and Tanabe, K., *J. Phys. Chem.* **90**, 4794 (1986).
5. Tanabe, K., Misono, M., Ono, Y., and Hattori, H., *in* Studies in Surface Science, Vol. 1. "New Solid Acids and Bases: Their Catalytic Properties," Elsevier, Amsterdam, 1989.
6. Arata, K., and Hino, M., *in* "Proceedings, 9th International Congress on Catalysis, Calgary, 1988" (M. J. Phillips and M. Ternan, Eds.), 1727. Chem. Institute of Canada, Ottawa, 1988.
7. Hino, M., and Arata, K., *J. Chem. Soc. Chem. Commun.* 1259 (1988).
8. Wadlinger, R. L., Kerr, G. T., and Rosinki, E. J., U.S. Patent 3,308,069, assigned to Mobil Oil Corporation, 1967.
9. Silver, R. G., Hou, C. J., and Ekerdt, J. G., *J. Catal.* **118**, 400 (1989).
10. Lange, F. F., *J. Am. Ceram. Soc.* **69**, 240 (1986).
11. Lange, F. F., *J. Mater. Sci.* **17**, 255 (1982).
12. Mercera, P. D. L., Ph.D. Thesis, University of Twente, 1991 ISBN 90-9004189-3, and references therein.
13. Garvie, R. C., *J. Phys. Chem.* **82**, 28 (1978).
14. Belloum, M., Travers, Ch., and Bournonville, J. P., *Rev. Inst. Fr. Petr.* **46**(1), 89 (1991).
15. Boudart, M., and Djéga-Mariadassou, *in* "Kinetics of Heterogeneous Catalytic Reactions," p. 6. Princeton Univ. Press, Lawrenceville, NJ, 1984.
16. Weitkamp, J., Jacobs, P. A., and Martens, J. A., *Appl. Catal.* **8**, 123 (1983).
17. Buchanan, J. S., Santiesteban, J. G., and Haag, W. O., *J. Catal.* **158**, 279 (1996).
18. Mills, G. A., Boedeker, E. R., and Oblad, A. G., *J. Am. Chem. Soc.* **72**, 1554 (1950).
19. Benesi, H. A., and Winquist, B. H. C., "Advances in Catalysis" (D. D. Eley, P. W. Selwood, and P. B. Weisz, Eds.), Vol. 27, p. 97. Academic Press, New York, 1978.
20. Olah, G. A., Prakash, G. K. S., and Sommer, J., *in* "Superacids." Wiley, New York, 1985.
21. Brown, H. C., and Johanneson, R. B., *J. Am. Chem. Soc.* **75**, 16 (1953).
22. Jacobs, P. A., and Heylen, C. F., *J. Catal.* **34**, 267 (1981).
23. Haag, W. O., Lago, R. M., and Weis, P. B., *Nature* **309**, 589 (1984).
24. Haw, J. F., Nicholas, J. B., Xu, T., Beck, L. W., and Ferguson, D. B., *Acc. Chem. Res.* **29**, 259 (1996).
25. Umansky, B., Engelhardt, J., and Hall, W. K., *J. Catal.* **127**, 128 (1991).
26. Tabora, J. E., and Davis, R. J., *J. Am. Chem Soc.* **118**, 12240 (1996).
27. Defosse, C., and Canesson, P., *React. Kinet. Catal. Lett.* **3**, 161 (1975).
28. Defosse, C., and Canesson, *J. Chem. Soc. Faraday Trans.* **1**, 2565 (1976).
29. Borade, R., and Clearfield, A., *J. Phys. Chem.* **96**, 6729 (1992).
30. Guimon, C., Zouiten, A., Boreave, A., Pfister-Guillouzo, G., Schulz, P., Fitoussi, F., and Quet, C., *J. Chem. Soc. Faraday Trans.* **90**, 3461 (1994).
31. Borade, R., Sayari, A., Adnot, A., and Kaliaguine, S., *J. Phys. Chem.* **94**, 5989 (1990).
32. Santiesteban, J. G., Natal-Santiago, M. A., Vartuli, J. C., and Chang, C. D., submitted for publication.
33. Soled, S., Murrell, L. L., Wachs, I. E., McVicker, G. B., Sherman, L. G., Chan, S., Dispenziere, N. C., and Baker, R. T. K., *in* "ACS Symposium Series 279: Solid State Chemistry in Catalysis" (R. K. Graselli and J. F. Brazdil, Eds.), p. 165, Am. Chem. Soc., Washington, DC, 1985.
34. Arata, K., "Advances in Catalysis" (D. D. Eley, P. W. Selwood, and P. B. Weisz, Eds.), Vol. 37, p. 165. Academic Press, New York, 1990.
35. Afanasiev, P., Geantet, C., Breysse, M., Coudurier, G., and Vedrine, J. C., *J. Chem. Soc. Faraday Trans.* **90**, 193 (1994).
36. Ogata, E., Kamiya, Y., and Ohta, N., *J. Catal.* **29**, 296 (1973).
37. Davis, B. H., *J. Catal.* **55**, 1704 (1978).
38. Gobal, F., *J. Chem. Res. (S)*, 182 (1980).
39. Iglesia, E., Barton, D. G., Soled, S. L., Moseo, S., Baumgartner, J. E., Gates, W. E., Fuentes, G. A., and Meitzner, G. D., *in* "Proceedings, 11th International Congress on Catalysis," *Stud. Surf. Sci. Catal.* **101**, 533 (1996).